Changes in ceramide metabolism are essential in Madin-Darby Canine Kidney cell differentiation

Lucila Gisele Pescio[1,2], Bruno Jaime Santacreu[1,2], Vanina Gisela Lopez[3], Carlos Humberto Paván[3], Daniela Judith Romero[1], Nicolás Octavio Favale[1,2], Norma Beatriz Sterin-Speziale[3,*]

[1]Universidad de Buenos Aires. Facultad de Farmacia y Bioquímica. Cátedra de Biología Celular y Molecular. Buenos Aires, Argentina

[2]CONICET - Universidad de Buenos Aires. Instituto de Química y Fisicoquímica Biológicas (IQUIFIB). Buenos Aires, Argentina

[3]CONICET - Universidad de Buenos Aires. Instituto de Química y Fisicoquímica Biológicas (IQUIFIB). LANAIS PROEM. Buenos Aires, Argentina

[*] To whom proofs and correspondence should be sent:
Prof. Norma Sterin-Speziale,
CONICET - Universidad de Buenos Aires. Instituto de Química y Físico-Química Biológica (IQUIFIB). LANAIS PROEM. Junín 956, 1113 Ciudad de Buenos Aires, Argentina.
Telephone: (5411) 4964-8291; Fax: (5411) 4962-5457; E-mail: speziale@ffyb.uba.ar

Running title: Sphingolipids and cell differentiation

Authors:

Lucila Gisele Pescio	lucilagpescio@ffyb.uba.ar
Bruno Jaime Santacreu	bsantacreu@ffyb.uba.ar
Vanina Gisela López	vanina.lopez@yahoo.com.ar
Carlos Humberto Paván	cpavan@qb.ffyb.uba.ar
Daniela Judith Romero	djromero@docente.ffyb.uba.ar
Nicolás Octavio Favale	nofaval@ffyb.uba.ar
Norma Beatriz Sterin-Speziale	speziale@ffyb.uba.ar

Abbreviations: Cer, ceramide; GlcCer, glucosylceramide; LacCer, lactosylceramide; SM, sphingomyelin; CerS, ceramide synthase; GSLs, glycosphingolipids; MDCK, Madin-Darby Canine Kidney; FB1, Fumonisin B1; CS, L-cycloserine; A, amitriptyline; I, isotonicity; H, hypertonicity; DHB, 2,5-Dihydroxybenzoic acid; SPT, serine palmitoyltransferase; CERT, ceramide transfer protein; aSMase, acid sphingomyelinase; siRNA, small interfering RNA

Abstract

Ceramides and complex sphingolipids with defined acyl-chain lengths play important roles in numerous cell processes. Six ceramide synthase isoenzymes (CerS1-6) are the key enzymes responsible for the production of the diversity of molecular species. In this study, we investigated the changes in sphingolipid metabolism during the differentiation of Madin-Darby Canine Kidney (MDCK) cells. By MALDI TOF TOF MS, we analyzed the molecular species of ceramide (Cer), glucosylceramide (GlcCer), lactosylceramide (LacCer) and sphingomyelin (SM) in non-differentiated and differentiated cells (cultured under hypertonicity). The molecular species detected were the same, but cells subjected to hypertonicity presented higher levels of C24:1 Cer, C24:1 GlcCer, C24:1 SM and C16:0 LacCer. Consistently with the molecular species, MDCK cells expressed CerS2, CerS4 and CerS6, but with no differences during cell differentiation. We next evaluated the different synthesis pathways with sphingolipid inhibitors and found that cells subjected to hypertonicity in the presence of amitriptyline, an inhibitor of acid sphingomyelinase, showed decreased radiolabeled incorporation in LacCer and cells did not develop a mature apical membrane. These results suggest that hypertonicity induces the endolysosomal degradation of SM, generating the Cer used as substrate for the synthesis of specific molecular species of glycosphingolipids that are essential for MDCK cell differentiation.

Keywords: ceramide, sphingolipids, glycolipids, mass spectrometry (MS), kidney, hypertonicity, ceramide synthase, cell differentiation

Introduction

Sphingolipids are a large and diverse class of lipids that possess important bioactive properties and control a myriad of cellular and physiological programs (1). Ceramide (Cer) is the precursor of complex sphingolipids such as glycosphingolipids (GSLs) and sphingomyelin (SM), and is considered an important intracellular signaling molecule involved in regulating differentiation, proliferation and apoptosis (2, 3). Cer is synthetized *de novo* in the endoplasmic reticulum by a series of reactions that begin with the condensation of L-serine and palmitoyl CoA by serine palmitoyl transferase (4). The resulting product, 3-ketosphinganine, is then reduced to form dihydrosphingosine by 3-ketosphinganine reductase. Dihydrosphingosine is further acylated by (dihydro)ceramide synthases (CerSs) to form dihydroceramide, and subsequent reduction of dihydroceramide to Cer by dihydroceramide desaturase (5). Cer is also produced from the recycled sphingosine formed by the breakdown of complex sphingolipids (salvage pathway). Therefore, CerSs control both the *de novo* synthesis and the salvage pathway of sphingolipids. In mammals, six CerS isoforms (CerS1-6), which display a cell type- or tissue-specific expression pattern, have been identified (6). Each CerS has a preference for a unique range of acyl-CoAs with particular acyl chain length. CerS1 uses C18-CoA; CerS2 uses C22 to C26-CoA; CerS3 exhibits a broad substrate specificity (C18 to C24-CoA); CerS4 also appears to have a broad range of specificity with a preference for C18-CoA and C20-CoA; and CerS5 and CerS6 use C14-CoA and C16-CoA (6-11). Therefore, the different substrate specificities of the individual CerS isoforms contribute to the fatty acid chain-length diversity of Cer and complex sphingolipid species in mammalian cells (12). It is now recognized that the different molecular species of Cer possess different biological functions and it appears that only a specific subset of Cers are involved in the control of certain processes. This subset of Cers may be defined by location, enzymes, chain length and/or biosynthetic pathway (13).

We have previously demonstrated that during the differentiation of Madin-Darby Canine Kidney (MDCK) cells induced by hypertonicity, cells develop a program of sphingolipid metabolism that includes an increase in GSL and SM synthesis (14, 15). This increased production of GSLs is essential to acquire the MDCK differentiated phenotype, reflected by the development of the mature apical membrane

domain and the formation of the primary cilium, considered the last steps in the final epithelial cell differentiation. We observed that the induction of differentiation evoked a Fumonisin B1 (FB1)-resistant increase in Cer that served as a precursor for the pool of GSLs involved in the final MDCK cell differentiation (14). These previous observations led us to wonder about the possibility that MDCK cell differentiation could be associated with the formation of specific molecular species of Cer that address the formation of the specific pool of GSLs. Consequently, the aim of the present work was to investigate the changes in the sphingolipid profile that are essential for MDCK cell differentiation and the pathways displayed by cells to achieve this optimal combination of molecular species of sphingolipids.

Materials and Methods

Cell culture. MDCK cells from American Type Culture Collection (2 x 10^5/35 mm dish) were grown in DMEM/F-12 (Invitrogen) supplemented with 10% FBS, penicillin (100 µg/ml) and streptomycin (100 µg/ml) at 37 °C in a humidified 5% CO_2 atmosphere. After 24 h, the medium was replaced by DMEM/F12 containing 0.5% FBS and incubated for another 24 h to reach confluence. Then, cells were kept under isotonicity or switched to a hypertonic medium (300 mM NaCl) and incubated for 24 or 48 h in the presence or absence of Fumonisin B1 20 µM (Sigma). After treatments, cells were trypsinized and counted by the trypan blue exclusion procedure.

Transfection with small interference RNA (siRNA). MDCK cells (2 x 10^5/35 mm dish) were grown in DMEM/F-12containing 10% FBS without antibiotics for 24 h. Then, cells were cultured in DMEM/F12 containing 0.5% FBS and transfected with 25 nM double-stranded siRNAs for acid sphingomyelinase or scrambled sequence (SCR) using HiPerFect Transfection Reagent (Qiagen) according to the manufacturer's instructions. After 24 h, transfection reagents were washed out and the medium was replaced by DMEM/F12 containing 1% FBS and incubated in the presence or absence of 300 mM NaCl for 48 h. The sequences of siRNAs for acid sphingomyelinase were 5´ UGGAAUUAUUACCGGAUUGUAdTdT 3´ (sense) and 5´ UACAAUCCGGUAAUAAUUCCAdTdT 3´ (antisense) and the sequences for SCR were 5´ CAGUCGCGUUUGCGACUGG 3´ (sense) and 5´ CCAGUCGCAAACGCGACUG 3´ (antisense).

Lipid extraction and preparation of sphingolipids. The cells were washed with phosphate-buffered saline (PBS) and transferred into 13 x 100 mm borosilicate tubes with Teflon-lined cap. After adding 0.5 ml of methanol and 0.25 ml of chloroform, the tubes were sonicated in a bath- type sonicator until they appeared dispersed. This single phase mixture was incubated at 48 °C overnight in a heating block. After cooling, 75 µl of 1 M KOH in methanol was added and incubated for 2 h at 37°C to cleave potentially interfering glycerolipids. After cooling at room temperature, approximately 6 µl of glacial acetic acid was

added to bring the pH near neutral. Then, 1 ml of chloroform and 2 ml of water were added and centrifuged to separate the phases. The lower phase was extracted and the solvent evaporated under N_2 atmosphere (16).

MALDI MS positive ion spectra of sphingolipids are normally dominated by SM because the sensitivity to molecules with quaternary ammonia groups. To overcome this problem and to be able to detect all species, a previous separation of the total extract into individual sphingolipid subclasses is unequivocally necessary (17). Because of that, sphingolipids were separated by thin-layer chromatography (TLC). Aliquots of the lipid extracts were dissolved in chloroform and spotted onto a TLC plate (Merck) and developed in two solvent systems: first in butanol:acetic acid:water (60:20:20 vol/vol/vol, Solvent 1), then the TLC plate was cut above the band corresponding to the dihydrosphingosine standard, and the top portion was run in Solvent 2 (chloroform:methanol 50:1.5 vol/vol). For SM analysis, the TLC was developed in chloroform:methanol:acetic acid:water (40:10:10:1 vol/vol/vol/vol). The plates were revealed by primuline staining and visualized under UV light (18). The bands corresponding to Cer, GlcCer, LacCer and SM were scraped off the TLC according with the standards references and the lipids were separated from the silica by extraction. This was performed by three successive extractions with chloroform:methanol:water (5:5:1 by vol), thoroughly mixing, centrifuging, collecting the solvents, and partitioning with 4 vol of water to recover the lipids in the chloroform phase (19). This phase was evaporated under N_2 flow and the samples were prepared for MALDI TOF-TOF analysis. The lipid standards were C12:0 SM (d18:1/12:0; N-lauroyl-D-erythro-sphingosylphosphorylcholine), C12:0 Cer (d18:1/12:0; N-lauroyl-D-erythrosphingosine), C18:0 GlcCer (d18:1/18:0; D-glucosyl-ß-1,1' N-stearoyl-D-erythro-sphingosine) and C12:0 LacCer (d18:1/12:0; D-lactosyl-ß-1,1' N-laurosyl-D-erythro-sphingosine), all from Avanti Polar Lipids, and DL-Dihydrosphingosine from Sigma.

MALDI TOF TOF mass spectrometry. Each sample obtained from the above procedure was cleaned by using micro-adsorptive C18 pipette ZipTips (Millipore) as manufacturer's instructions. Two microliters of each eluated sample were mixed with 2 µl of matrix solution (20 mg/ml 2,5-Dihydroxybenzoic acid

(DHB, Sigma) in Methanol:TFA (90:0.1 vol/vol) with 100mM $(NH_4)_2SO_4$). The mixture was directly spotted onto the sample plate and air-dried. All mass spectrometric analyses were performed in LANAIS-PROEM–CONICET-Argentina using a 4800 MALDI TOF/TOF™ Analyzer (Applied Biosystems) equipped with a ND:YAG laser (355 nm) in positive ion mode. All mass spectrometric data were acquired and analyzed using Data Explorer software. Conditions: Acceleration voltage: Grid to sourse 1 0.8050/ Mirror 2 to Mirror 1 1.4611/ Mirror 2 to sourse 1 1.0900. Sourse 1 20KVolts. Delayed extraction time: 330 nanoseconds. Typical ppm error: 50-80 ppm.

Labeling of sphingolipids. Sphingolipids were labeled by feeding MDCK cells with D- [1-^{14}C]galactose (2 µCi/ml, American Radiolabeled Chemicals) for 5 h before trypsinization and extracted as described above. In the short term incubation, the inhibitors (amitriptyline 30 µM, amitriptyline 30 µM in addition to L-cycloserine (CS) 0.5 mM or amitriptyline 30 µM in addition to Fumonisin B1 20 µM), were added 1 h before [^{14}C]galactose (total inhibitors incubation: 6 h), and in long term incubation the inhibitors were added 1 h before the addition of the hypertonic medium (total inhibitors incubation: 49 h). Extracted sphingolipids were spotted onto a TLC plate, developed in chloroform/methanol/0.22% $CaCl_2$ (60:35:8; vol/vol/vol) and visualized by autoradiography. The corresponding radioactive spots were scraped off the TLC plates for additional measurement by liquid scintillation counting. Data were normalized to the number of counts incorporated every 10^6 cells.

Reverse transcription-PCR. Total RNA was extracted using the SV total RNA isolation system (Promega) in accordance with the manufacturer's instructions. Equal amounts of RNA (500 ng) were used to synthesize the first-strand cDNA using the reverse transcriptase system and then PCR. Primers used for PCR were 5´ TCAGTGCAATTGGTGGAAAA3´ (forward) and 5´ ACCTTGAGCGGAAACCAGTA 3´ (reverse) for CerS1, 5´ CCCACCTTGGAGCATTTCTA 3´ (forward) and 5´ TCGGGTGATGATGAAGACAA 3´ (reverse) for CerS2, 5´GATTTTGGCTTCCTCCAACA 3´ (forward) and 5´ GGGGTAGCCATTCCATACCT 3´ (reverse) for CerS3, 5´ TCCTACAGCTCCAACCTGCT 3´ (forward) and 5´ CTGGGCAATGGAGTCGTAGT 3´

(reverse) for CerS4, 5´ GTTCTGGGACATCCGACAGT 3´ (forward) and 5´ TGAGCTGCTTTCCACATCAC 3´ (reverse) for CerS5, 5´TAGCCAAACCATGTGCCATA 3´ (forward) and 5´ TGCCTTGTATTCCACAACCA 3´ (reverse) for CerS6, and 5´ ACCACAGTCCATGCCATCAC 3´ (forward) and 5´ ATGTCGTTGTCCCACCACCT 3´ (reverse) for GAPDH. RT-PCR products were resolved on 2% agarose-gels.

Real Time-PCR. Relative quantitative real-time PCR was performed on a Rotor-Gene Q real-time PCR using cDNA, new set of primers and Real-Mix (Biodynamics) according to the manufacturer's instructions. Primers used for Real Time PCR were 5´ CGTCTTTGCCATTGTCTTCA 3´ (forward) and 5´ CAGCTGTAGCACTCCCATCA 3´ (reverse) for CerS2, 5´ CTGAAACCGGCCCTGTACTA 3´ (forward) and 5´ GCAGGTTGGAGCTGTAGGAG 3´ (reverse) for CerS4 and 5´ GCCCTCAATGACCACTTTGT 3´ (forward) and 5´ CTCCTTGGAGGCCATGTAGA 3´ (reverse) for GAPDH.

Confocal immunofluorescence microscopy. MDCK cells grown on coverslips were cultured as described above in hypertonic medium in the presence or absence of amitriptyline 30 μM, L-cycloserine 0.5 mM or Fumonisin B1 20 μM. The inhibitors were added 1 h before subjection to hypertonicity. After 48 h of treatment, cells were fixed in 4% paraformaldehyde for 20 min and permeabilized with 0.1% (v/v) Triton X-100 for 20 min. After blocking, cells were incubated for 90 min with 1:10 of mouse anti-gp135 (kindly donated by Dr. Ojakian) and 1:2000 of rabbit anti-α catenin (Sigma) at room temperature. Primary interactions were detected by using anti-rabbit FITC and anti- mouse TRICT – conjugated antibodies (Jackson Immunoresearch). After 60 min, the coverslips were mounted onto microscope glass slides with Vectashield Mounting Medium (Vector Laboratory). Images were obtained by an Olympus FV300 confocal microscope (model BX61) equipped with Ar and He–Ne lasers, and oil immersion 60× objective with numerical aperture 1.4. Images were taken with the acquisition software FluoView version 3.3, and the software Image-Pro plus version 4.5 was used for image analysis.

Results

Changes in the sphingolipid profile during MDCK cell differentiation

We have previously demonstrated that hypertonicity induces a specific program of sphingolipid metabolism that includes an increase in GSL synthesis that is essential for MDCK cell differentiation (14). We now investigated the molecular species of Cer, GlcCer, LacCer and SM involved in this process. The determinations were achieved by MALDI TOF TOF MS. MDCK cells were cultured under isotonicity (control) or hypertonicity for 24 h or 48 h, trypsinized and the sphingolipids were extracted as described by Merrill et al. (16) and separated by TLC. If the TLC was developed with butanol:acetic acid:water (60:20:20 vol:vol:vol) as solvent system, Cer migrated near the front run, thus being difficult to distinguish Cer molecular species from the interferences. To overcome this difficulty, we performed a one-dimension – two-step TLC, as described in "Materials and Methods". Figure 1 shows representative TLC plates of the first and the second step of TLC development. The comparison with the standards shows that the bands corresponding to SM and LacCer were in the bottom portion, while the bands of Cer and GlcCer were in the top portion. These bands were scrapped off and the lipids were extracted from the silica gel and analyzed by MALDI TOF TOF MS. The identity of each sphingolipid was confirmed by MS/MS. Characteristic fragmentation patterns were observed for Cer (m/z 264: sphingosine – $2H_2O$, m/z 282: sphingosine – H_2O), GlcCer (m/z 264 and 282, $[M+H]^+$ - Glucose, $[M+H]^+$ – (Glucose + H_2O)) and LacCer (m/z 264 and 282, $[M+H]^+$ - (LacCer + H_2O)).

Figure 2a shows representative mass spectra of isolated Cer, GlcCer and LacCer. Peaks at m/z 550.6 and 522.6 corresponded to dimethyldioctadecylammonium ion and a related species, respectively; which are described as common contaminants in mass spectrometry (20). In addition to the $[M+H]^+$ of Cer, GlcCer and LacCer species, mass spectra showed the corresponding $[M+H – H_2O]^+$ and $[M+Na]^+$ adducts. $[M+K]^+$ adducts were almost eliminated by the use of Zip Tips. The Cer spectrum was enlarged at m/z 510-690, the GlcCer spectrum at m/z 680-850 and the LacCer spectrum at m/z 840-1010, to visualize the $[M+H]^+$, $[M+H – H_2O]^+$ and $[M+Na]^+$ ions of the subspecies of the corresponding sphingolipid (Supplemental Figure S1). The main species of Cer, GlcCer and LacCer found are listed in Table 1, which

shows the m/z of $[M+H]^+$, $[M+H - H_2O]^+$ and $[M+Na]^+$ ions of the molecular species detected, and in the left part of each column includes the corresponding predicted monoisotopic mass. The identity of d18:1 was provided by MS/MS analyses, by the detection of fragments at m/z 264 (sphingosine – $2H_20$). We detected six major subspecies of Cer: d18:1/C16:0, d18:1/C18:0, d18:1/C20:0, d18:1/C22:0, d18:1/C24:1 and d18:1/C24:0. Mass spectra and Table 1 show the molecular species of GlcCer and LacCer with the same Cer backbone as the free Cers. Note that the $[M+H]^+$ ions of some species of LacCer were not observed. These evidences are in accordance with previous reports that showed that, using DHB as matrix, neutral oligosaccharides render preferentially sodiated ions $[M+Na]^+$ (21, 22).

The relative composition of the molecular species of Cer, GlcCer and LacCer in MDCK cells cultured under isotonicity (undifferentiated) or hypertonicity for 24 h and 48 h (differentiated) is shown in Fig. 3. The relative composition of the subspecies of each sphingolipid was calculated based on the peak heights of the mass spectra. While $[M+H - H_2O]^+$ ions represented a major ion from Cer molecular species (m/z 520.61, 630.74, 632.76), $[M+Na]^+$ adducts represented a major ion from GlcCer (m/z 722.77, 832.92, 834.94) and LacCer species (m/z 884.72, 994.84, 996.86) (Fig. 2 and Supplemental Fig. S1). Moreover, LacCer mass spectra showed prominent peaks at m/z corresponding to the mass of dehydrated Cer backbone from LacCer subspecies (Fig. 2a), probably generated by insource fragmentation. For the reason mentioned above, to calculate the percentage of each subspecies, we considered the addition of the peak height of $[M+H]^+$, $[M+H - H_2O]^+$, $[M+Na]^+$ adducts and the height of dehydrated Cer (for GlcCer and LacCer molecular species).

In the three conditions analyzed, we detected the same six major subspecies of Cer, GlcCer and LacCer, but the MS profiles showed some differences. C16:0 Cer, C24:0 Cer and C24:1 Cer were the predominant species both in control MDCK cells and in cells subjected to hypertonicity. However, cells subjected to hypertonicity showed a different relative proportion of Cer molecular species. Over 24 h of treatment, the percentage of C16:0 Cer increased while the percentage of C18:0 Cer decreased, whereas over 48 h of treatment, the percentage of C24:1 Cer increased. Cells subjected to hypertonicity also showed a progressive increase in the percentages of C24:0 and C24:1 GlcCer, while the percentage of C18:0

GlcCer was about 4% in control cells and did not change in cells subjected to hypertonicity. The enrichment of the C24 GlcCer species seemed to occur at expense of a slight decrease in both C16:0 and C22:0 GlcCer. The LacCer profile showed a low percentage of C18:0 LacCer in either experimental condition, with an increase in C24:1 LacCer at 24 h of hypertonicity and a further increase in C16:0 LacCer after 48 h of hypertonicity (Fig. 3).

We have previously described that, after 24 h of hypertonicity, synthesis of GlcCer is increased and that, after 48 h of treatment, synthesis of LacCer is increased and GlcCer levels return to control values (14). In this work, results from mass spectrometry showed that besides the changes in GlcCer and LacCer levels, hypertonicity also evoked changes in the relative amount of each molecular species, thus favoring the formation of C24:0 and C24:1 but not of C18:0 GlcCer or LacCer. These results show that the sphingolipid profile of MDCK cells is modified during the progression of cell differentiation.

In a recent work, we have demonstrated that SM metabolism is also involved in the differentiation of MDCK cells induced by hypertonicity (15). In this work, we were interested in analyzing the molecular species of SM in undifferentiated and differentiated MDCK cells. A representative mass spectrum of isolated SM is shown in Fig. 4A. SM ions were easily identified, since the mass spectra showed higher peaks corresponding to the molecular species of SM and shorter background peaks. SM spectra showed peaks corresponding to $[M+H]^+$ ions, and a lower proportion of $[M+Na]^+$ ions. The most abundant $[M+H]^+$ ion was at m/z 703.7 corresponding to C16:0 SM, which accounted for 76% of all the SM molecular species in control cells (Fig. 4Aa). The spectrum was enlarged at m/z 650 – 850 for better visualization of the SM peaks (Fig. 4Ab). Fragmentation of SM in positive mode leads to the formation of an ion at m/z 184, characteristic of the phosphocholine polar head, thus confirming SM identity. The MS/MS spectrum of m/z 703.7 is shown in Fig. 4Ac. Figure 4B shows the relative composition of the subspecies of SM from cells cultured under isotonicity or hypertonicity for 48 h. Although cells cultured under hypertonicity also showed C16:0 SM as the predominant molecular species, these cells were significantly enriched in C24:1 and C24:0 SM. The percentage of C18:0 SM was very low (about 4%) both in cells cultured under isotonicity and in cells cultured under hypertonicity. Minor changes were

observed in other subspecies of SM. These results show that although C16:0 SM is the prevalent species of SM in both undifferentiated and differentiated MDCK cells, a clear increase in C24:0 and C24:1 SM is observed during cell differentiation. We next asked about the origin of such changes in the profile of sphingolipid molecular species.

Ceramide synthase expression in MDCK cells during differentiation

Since it is accepted that the presence of the various sphingolipid molecular species is due to the activity of CerSs with different fatty acyl CoA affinity, we further studied CerS expression in both experimental conditions. For that purpose, we designed primers for the six isoforms of CerS (CerS1-6) from MDCK cells based on the predicted sequences found at GenBank. Then, we analyzed the expression of the different CerSs in cells subjected to isotonicity and hypertonicity. First, we performed a RT-PCR with 40 cycles, to guarantee the detection of the expression of all isoforms. MDCK cells expressed CerS2, CerS4 and CerS6, but not CerS1, CerS3 and CerS5 (Fig. 5A). Next, we analyzed the expression of these three isoforms in the adjusted conditions to detect changes in mRNA expression. The mRNA expression of CerS2, CerS4 and CerS6 in cells subjected to isotonicity was not significantly different from that in cells subjected to hypertonicity (Fig. 5B and C). Then, we performed a quantitative analysis of the gene expression of these enzymes by Real Time PCR. For this assay, we designed other primers to obtain shorter amplicons, more suitable for this reaction. Results from Real Time PCR demonstrated no quantitative differences, thus confirming the results obtained by RT-PCR (Fig. 5D). Taken together, these results demonstrate that MDCK cells express three isoforms of CerS: CerS2, CerS4 and CerS6, which are not regulated by hypertonicity. Since we have previously found that MDCK cell differentiation induced by hypertonicity is resistant to FB1 (14), we hypothesized that hypertonicity could induce the activation of a CerS insensitive to FB1, whose product, a specific pool of Cer, could serve for the synthesis of the GSLs required for MDCK cell differentiation. To elucidate whether FB1 regulates the expression of any of the CerS isoforms, we analyzed the mRNA of CerS1-6 in cells subjected to hypertonicity in the presence of FB1. RT-PCR with 40 cycles showed that the same three CerS isoforms were expressed in cells subjected to hypertonicity either in the presence or absence of FB1 (Fig. 5A), and when we

compared the gene expression of CerS2, CerS4 and CerS6 no significant changes were found (Fig. 5 B-D). These results suggest that the FB1 resistance in MDCK cells subjected to hypertonicity is not due to changes in the expression of any CerS isoform.

Then, we analyzed by MALDI TOF TOF MS the molecular species of GlcCer in cells subjected to hypertonicity treated or not with FB1.The analysis showed that the presence of FB1 did not evoke changes in the GlcCer profile in cells subjected to hypertonicity (Fig. 5E), thus demonstrating that FB1 did not exert any selective modification in the molecular species of GlcCer during MDCK cell differentiation.

A specific source of ceramide is necessary for the synthesis of the GSLs essential for MDCK cell differentiation

We have previously analyzed the contribution of the different pathways to GSL synthesis in MDCK cells, based on the use of L-cycloserine (CS) and FB1, metabolic inhibitors of serine palmitoyltransferase (SPT) and CerS, respectively (14). In that work, we reported that while the inhibition of GlcCer synthase abolishes apical membrane maturation, neither inhibition of SPT nor inhibition of CerS affect this process (14). It is accepted that besides the *de novo* (pathway 1) and salvage pathways (pathway 2), there is a third pathway known as direct glycosylation (pathway 3), where the source of Cer precursor is the endosomal degradation of SM, which can be further glycosylated in the Golgi complex. So, pathway 3 is defined as the one that includes transport of sphingolipids from endosomes/lysosomes to the Golgi, with no involvement of CerSs (23). To study the involvement of the endolysosomal degradation of SM in the differentiation of MDCK cells induced by hypertonicity, we used amitriptyline as acid sphingomyelinase inhibitor.

First, we checked the influence of pathway 3 on the acquisition of the differentiated phenotype, by performing immunofluorescence microscopy. To this end, cultured cells were treated with amitriptyline for 1 h before subjecting them to hypertonicity. In different experiments, cells were treated with CS (inhibitor of pathway 1) and FB1 (inhibitor of pathways 1 and 2) as controls (Fig. 6A). Three confocal planes were analyzed by using gp135 as a marker of apical membrane maturation and α catenin as

basolateral marker. As expected, we observed apical accumulation of gp135 in cells subjected to hypertonicity for 48 h, thus demonstrating the maturation of the apical membrane proper of differentiated cells. Neither inhibition of *de novo* synthesis (pathway 1) nor inhibition of the salvage pathway (pathway 2) altered the acquisition of the differentiated phenotype, while inhibition of pathway 3 evoked a profound alteration in the cell phenotype (Fig. 6A). At first, in amitriptyline-treated cells, gp135 appeared misplaced, since basal accumulation was observed in some cells. In the middle plane, amitriptyline-treated cells established their luminal domain at intercellular lumina between neighboring cells rather than at the apex, as denoted by the lateral lumina enriched in the apical marker gp135. The most apical plane showed no accumulation of gp135. Taken together, these results indicate that amitriptyline alters the polarized phenotype of MDCK cells, inducing a phenotype of intermediate polarity, as described previously by Cohen and collaborators (24). These results suggest an important role of acid sphingomyelinase in MDCK cell differentiation. Then, we transfected cells with siRNA to acid sphingomyelinase and control cells with scrambled siRNA, and we found that acid sphingomyelinase KD cells showed alteration of the development of the apical membrane, and similar to amitriptyline – treated cells, some cells exhibited lateral lumina with gp135 (Fig. 6B).

We hypothesize that acid sphingomyelinase is involved in a novel mechanism displayed by hypertonicity, that induces MDCK cells to produce a specific profile of GSLs necessary to the development of the apical membrane. In order to investigate the sphingolipid metabolism, we analyzed the incorporation of radiolabed precursors in cultured cells in the presence of amitriptyline and others sphingolipid synthesis inhibitors. We designed two protocols including a 5-h incubation with [^{14}C]galactose before trypsinization, with two different periods of incubation with the inhibitors. To elucidate whether pathway 3 is active in differentiated cells, we added amitriptyline 1 h before the incubation with the radiolabeled precursor (protocol 1 – short term). In protocol 2 (long term), the inhibitors were added 1 h before subjecting the cells to the hypertonic medium (total time of incubation with the inhibitors: 49 h).

In the short-term incubation with the inhibitors, treatment with amitriptyline did not modify the incorporation of [^{14}C]galactose to GlcCer in control cells or cells subjected to hypertonicity. When CS

was also added, almost 50% decrease was observed, thus reflecting the contribution of the *de novo* synthesis pathway. With respect to LacCer, in cells subjected to hypertonicity in the presence of amitriptyline, it levels significantly decreased and no additional decrease was observed with CS and FB1, thus demonstrating that LacCer synthesis occurs by pathway 3 after 48 h of hypertonicity. In the long-term incubation, amitriptyline-treated cells increased the incorporation of [^{14}C]galactose to GlcCer and LacCer in cells subjected to hypertonicity for 48 h. To test whether this effect is due to a compensatory increase in *de novo* synthesis, we studied sphingolipid metabolism in the presence of amitriptyline in addition to CS (A + CS). The results showed that CS induced a decrease in radiolabeled sphingolipids in almost all conditions, more clearly in the long-term incubation with the inhibitors (Fig. 7a). These results could indicate that, in the presence of amitriptyline, the *de novo* synthesis of sphingolipids increases probably as compensatory effect, but that the pool generated is not useful to reverse the effect of the absence of GSLs synthesized by pathway 3. The knock down of aSMase did not modify the incorporation of [^{14}C]galactose in cells incubated under isotonicity, while a decrease in [^{14}C]GlcCer was obtained in cells treated with CS and FB1 in the long term-incubation experiments. In contrast, aSMAse siRNA - transfected cells incubated under hypertonicity showed a significant decrease in [^{14}C]GlcCer and [^{14}C]LacCer, thus demonstrating the involvement of pathway 3. Treatment with CS or FB1 did not induce a greater inhibitory effect (Fig. 7b).

Taken together, we suggest that the GSLs necessary for the differentiation of MDCK cells are derived from endolysosomal degradation of SM by acid sphingomyelinase.

Discussion

We have previously reported that renal collecting duct cells regulate the branching of sphingolipid metabolism depending on the stage of cellular differentiation (25). Further, we demonstrated that, during hypertonicity-induced differentiation, MDCK cells develop a program of sphingolipid metabolism that includes a FB1-resistant increase in GSLs (14) and SM synthesis (15). Consequently, we hypothesized that different CerSs synthesizing different species of sphingolipids could play a role in the process of differentiation. However, in the present study, we found that the pattern of CerSs does not change during differentiation, while sphingolipid molecular species do change probably due to an activation of the so-called pathway 3, which does not require the involvement of CerSs. We found that MDCK cells expressed three of the six isoforms of CerS: CerS2, Cer4 and CerS6. These results are in accordance with the isoforms of CerS found in mouse kidneys (6), with the difference that mouse kidneys also express CerS5. MALDI TOF TOF MS allowed us to find six molecular species of Cer that correlate with the expression pattern of the various CerSs: C22:0 Cer, C24:0 Cer and Cer C24:1, which may be synthesized by CerS2; C18:0 Cer and C20:0 Cer which may be synthesized by CerS4; and C16:0 which may be synthesized by CerS6. While no changes were observed in the profile of molecular species during differentiation, changes were observed in their relative amount. First, we found that the Cer profile in non-differentiated MDCK cells (isotonicity) differed from that in the cells that were in the process of differentiation. An increase in C16:0 Cer was obtained after 24 h of hypertonicity (29% vs. 39%), concomitantly with a decrease in 18:0 Cer (15% vs. 5%). We suggest that this change in Cer molecular species is the starting point for the sphingolipid involvement in MDCK cell differentiation. Thus, after 24 h of hypertonicity, C16:0 Cer was the most abundant Cer and the main species of GlcCer, and, after 48 h of hypertonicity, it constituted most of the LacCer species. It is interesting to point out that after 48 h of hypertonicity C16:0 Cer decreased. We interpreted that this was due to the activation of GlcCer synthase under hypertonicity, as we have previously reported (14), which generates more C16:0 GlcCer to be further converted to C16:0 LacCer after 48 h of hypertonicity. We base this suggestion on our previous

study where we showed that GlcCer synthesis increases after 24 h of hypertonicity, declining thereafter, while LacCer increases after 48 h of hypertonicity. The lower percentage of C16:0 molecular species of Cer and GlcCer was compensated with an increase in the percentages of C24:0 Cer and C24:1 Cer species in cells subjected to hypertonicity. Such increase in C24:1 Cer is in agreement with a recent work describing C24:1 Cer as a promoter of primary cilium formation (26), since we have previously reported that, in our experimental conditions, MDCK cells acquired primary cilium at 48 h of hypertonicity.

We have previously shown that the synthesis of GSLs is necessary for the maturation of the apical membrane and the acquisition of primary cilium of renal collecting duct differentiated cells. It is known that the different fatty acids acylated in sphingoid bases bring about different properties to the sphingolipids that in turn define their function. A pioneer report of Simons et al. described that the mature apical membrane of epithelial cells is enriched in GSLs (27). We thus wondered why MDCK cells under isotonicity synthesize GSLs but do not show apical membrane maturation and cilium formation. Our present results allow us to suggest that a critical point could be the combination of the molecular species of Cer, GlcCer and LacCer, where higher levels of C24:1 Cer must be accompanied by lower levels of C16:0 GlcCer and a higher proportion of C16:0 LacCer than in the non-differentiated state.

Since we failed to obtain differences in the profile of CerSs and cell differentiation was not affected by the inhibition of the *de novo* synthesis or the salvage pathways, we attempted to find out the origin of such molecular species. So, we focused our attention on SM and its degradation pathway. We found that, under isotonicity, C16:0 SM constituted 76% of total SM, consistent with the specificity of the ceramide transfer protein (CERT) to transport C16:0 Cer. In the differentiated state, over 48 h of hypertonicity, the percentage of C16:0 SM was almost 50% lower, having a profile quite similar to that of LacCer in the same experimental condition. Thus, we hypothesized that SM hydrolysis could constitute the real starting point of the metabolic pathway involved in the process. In fact, we found that the inhibition of acid sphingomyelinase with amitriptyline or the knock down of the enzyme disrupted apical membrane development. Moreover, both strategies induced a decrease in the levels of [^{14}C]GSLs over 48 h of hypertonicity. Consistent with our findings, the importance of the Cer derived from endolysosomal

degradation of SM by acid sphingomyelinase has been also pointed out by He et al., who characterized an apical ceramide-enriched compartment that regulates the ciliogenesis of MDCK cells (28).

In summary, this study provides experimental evidences that the differentiation of MDCK cells requires changes in Cer metabolism to achieve a specific profile of molecular species of GlcCer and LacCer essential for MDCK cell differentiation. The results suggest that this special pool of Cer is produced by hydrolysis of SM by acid sphingomyelinase during MDCK cell differentiation.

Acknowledgements: We greatly appreciate the gift of gp135 mouse hybridoma supernatant from Dr. Ojakian (SUNY Downstate Medical Center, USA). We would like to give our thanks to Roberto Fernandez for confocal microscope technical assistance and to LANAIS-PROEM–CONICET-Argentina for the mass spectrometry assistance.

Sources of funding: The work was supported by grants UBACyT 20020100100609 and 20020150200079 from Universidad de Buenos Aires, PIP 11220110100413 from Consejo Nacional de Investigaciones Científicas y Técnicas (CONICET) and PICT 1038 and 1625 from Agencia Nacional de Promoción Científica y Tecnológica (ANPCyT), Argentina.

Disclosures: None relevant to this study.

References

1. Hannun, Y. A., and L. M. Obeid. 2008. Principles of bioactive lipid signalling: lessons from sphingolipids. *Nat Rev Mol Cell Biol* **9**: 139-150.

2. Pettus, B. J., C. E. Chalfant, and Y. A. Hannun. 2002. Ceramide in apoptosis: an overview and current perspectives. *Biochim Biophys Acta* **1585**: 114-125.

3. Kolesnick, R. 2002. The therapeutic potential of modulating the ceramide/sphingomyelin pathway. *J Clin Invest* **110**: 3-8.

4. Hanada, K. 2003. Serine palmitoyltransferase, a key enzyme of sphingolipid metabolism. *Biochim Biophys Acta* **1632**: 16-30.

5. Futerman, A., and H. Riezman. 2005. The ins and outs of sphingolipid synthesis. *Trends Cell Biol* **15**: 312-318.

6. Laviad, E. L., L. Albee, I. Pankova-Kholmyansky, S. Epstein, H. Park, A. H. Merrill, and A. H. Futerman. 2008. Characterization of Ceramide Synthase 2. *Journal of Biological Chemistry* **283**: 5677-5684.

7. Venkataraman, K., C. Riebeling, J. Bodennec, H. Riezman, J. C. Allegood, M. C. Sullards, A. H. Merrill, and A. H. Futerman. 2002. Upstream of Growth and Differentiation Factor 1 (uog1), a Mammalian Homolog of the Yeast Longevity Assurance Gene 1 (LAG1), RegulatesN-Stearoyl-sphinganine (C18-(Dihydro)ceramide) Synthesis in a Fumonisin B1-independent Manner in Mammalian Cells. *Journal of Biological Chemistry* **277**: 35642-35649.

8. Guillas, I., J. C. Jiang, C. Vionnet, C. Roubaty, D. Uldry, R. Chuard, J. Wang, S. M. Jazwinski, and A. Conzelmann. 2003. Human Homologues of LAG1 Reconstitute Acyl-CoA-dependent Ceramide Synthesis in Yeast. *Journal of Biological Chemistry* **278**: 37083-37091.

9. Riebeling, C., J. C. Allegood, E. Wang, A. H. Merrill, and A. H. Futerman. 2003. Two Mammalian Longevity Assurance Gene (LAG1) Family Members, trh1 and trh4, Regulate

Dihydroceramide Synthesis Using Different Fatty Acyl-CoA Donors. *Journal of Biological Chemistry* **278**: 43452-43459.

10. Mizutani, Y., A. Kihara, and Y. Igarashi. 2005. Mammalian Lass6 and its related family members regulate synthesis of specific ceramides. *Biochem J* **390**: 263-271.

11. Mizutani, Y., A. Kihara, and Y. Igarashi. 2006. LASS3 (longevity assurance homologue 3) is a mainly testis-specific (dihydro)ceramide synthase with relatively broad substrate specificity. *Biochem J* **398**: 531-538.

12. Pewzner-Jung, Y., S. Ben-Dor, and A. H. Futerman. 2006. When Do Lasses (Longevity Assurance Genes) Become CerS (Ceramide Synthases)? *Journal of Biological Chemistry* **281**: 25001-25005.

13. Mullen, T. D., Y. A. Hannun, and L. M. Obeid. 2012. Ceramide synthases at the centre of sphingolipid metabolism and biology. *Biochem J* **441**: 789-802.

14. Pescio, L., N. Favale, M. Marquez, and N. Sterin-Speziale. 2012. Glycosphingolipid synthesis is essential for MDCK cell differentiation. *Biochim Biophys Acta* **1821**: 884-894.

15. Favale, N. O., B. J. Santacreu, L. G. Pescio, M. G. Marquez, and N. B. Sterin-Speziale. 2015. Sphingomyelin metabolism is involved in the differentiation of MDCK cells induced by environmental hypertonicity. *J Lipid Res* **56**: 786-800.

16. Merrill Jr, A. H., M. C. Sullards, J. C. Allegood, S. Kelly, and E. Wang. 2005. Sphingolipidomics: High-throughput, structure-specific, and quantitative analysis of sphingolipids by liquid chromatography tandem mass spectrometry. *Methods* **36**: 207-224.

17. Schiller, J., R. Süß, J. Arnhold, B. Fuchs, J. Leßig, M. Müller, M. Petković, H. Spalteholz, O. Zschörnig, and K. Arnold. 2004. Matrix-assisted laser desorption and ionization time-of-flight (MALDI-TOF) mass spectrometry in lipid and phospholipid research. *Progress in Lipid Research* **43**: 449-488.

18. van Echten-Decker, G. 2000. Sphingolipid extraction and analysis by thin-layer chromatography. *Methods Enzymol* **312**: 64-79.

19. Oresti, G. M., J. G. Reyes, J. M. Luquez, N. Osses, N. E. Furland, and M. I. Aveldaño. 2010. Differentiation-related changes in lipid classes with long-chain and very long-chain polyenoic fatty acids in rat spermatogenic cells. *Journal of Lipid Research* **51**: 2909-2921.

20. Manier, M. L., D. S. Cornett, D. L. Hachey, and R. M. Caprioli. 2008. Identification of Dimethyldioctadecylammonium Ion (m/z 550.6) and Related Species (m/z 522.6, 494.6) as a Source of Contamination in Mass Spectrometry. *Journal of the American Society for Mass Spectrometry* **19**: 666-670.

21. Tanaka, K., M. Yamada, K. Tamiya-Koizumi, R. Kannagi, T. Aoyama, A. Hara, and M. Kyogashima. 2011. Systematic analyses of free ceramide species and ceramide species comprising neutral glycosphingolipids by MALDI-TOF MS with high-energy CID. *Glycoconj J* **28**: 67-87.

22. Stahl, B., M. Steup, M. Karas, and F. Hillenkamp. 1991. Analysis of neutral oligosaccharides by matrix-assisted laser desorption ionization mass spectrometry. *Analytical Chemistry* **63**: 1463-1466.

23. Gillard, B. K., R. G. Clement, and D. M. Marcus. 1998. Variations among cell lines in the synthesis of sphingolipids in de novo and recycling pathways. *Glycobiology* **8**: 885-890.

24. Cohen, D., P. J. Brennwald, E. Rodriguez-Boulan, and A. Müsch. 2004. Mammalian PAR-1 determines epithelial lumen polarity by organizing the microtubule cytoskeleton. *The Journal of Cell Biology* **164**: 717-727.

25. Facchinetti, M., C. Beuret, M. Marquez, and N. Sterin-Speziale. 2003. Differential branching of the sphingolipid metabolic pathways with the stage of development. Involvement of sphingosine kinase. *Biol Neonate* **84**: 243-251.

26. He, Q., G. Wang, S. Wakade, S. Dasgupta, M. Dinkins, J. N. Kong, S. D. Spassieva, and E. Bieberich. 2014. Primary cilia in stem cells and neural progenitors are regulated by neutral sphingomyelinase 2 and ceramide. *Molecular Biology of the Cell* **25**: 1715-1729.

27. Simons, K., and G. Van Meer. 1988. Lipid sorting in epithelial cells. *Biochemistry* **27**: 6197-6202.

28. He, Q., G. Wang, S. Dasgupta, M. Dinkins, G. Zhu, and E. Bieberich. 2012. Characterization of an apical ceramide-enriched compartment regulating ciliogenesis. *Molecular Biology of the Cell* **23**: 3156-3166.

TABLE 1

m/z values for sphingolipid species predicted (monoisotopic) and detected by MALDI TOF TOF MS

	M + H - H_20		M + H		M + Na	
	Exact mass	Detected	Exact mass	Detected	Exact mass	Detected
d18:1-C16:0 Cer	520.50935	520.61	538.51992	538.62	560.50189	560.61
d18:1-C18:0 Cer	548.54065	548.67	566.55122	566.73	588.53319	588.60
d18:1-C20:0 Cer	576.57190	576.69	594.58252	594.69	616.56449	616.69
d18:1-C22:0 Cer	604.60325	604.72	622.61382	622.73	644.59579	644.72
d18:1-C24:1 Cer	630.61890	630.74	648.62947	648.75	670.61144	670.74
d18:1-C24:0 Cer	632.63455	632.76	650.64512	650.76	672.62709	672.75
d18:1-C16:0 GlcCer	682.56218	682.76	700.57274	700.76	722.55472	722.77
d18:1-C18:0 GlcCer	710.59348	710.80	728.60404	728.86	750.58602	750.80
d18:1-C20:0 GlcCer	738.62478	738.82	756.63534	756.71	778.61732	778.85
d18:1-C22:0 GlcCer	766.65608	766.88	784.66664	784.84	806.64862	806.90
d18:1-C24:1 GlcCer	792.67173	792.90	810.68229	810.92	832.66427	832.92
d18:1-C24:0 GlcCer	794.68738	794.92	812.69794	812.92	834.67992	834.94
d18:1-C16:0 LacCer	844.6150	844.71	862.62557	862.73	884.60754	884.72
d18:1-C18:0 LacCer	872.6463	872.76	866.65687		912.63884	912.75
d18:1-C20:0 LacCer	900.6776	900.75	918.68817		940.67014	940.79
d18:1-C22:0 LacCer	928.7089	928.81	946.71947	946.84	968.70144	968.82
d18:1-C24:1 LacCer	954.7246	954.84	972.71512	972.84	994.71709	994.84
d18:1-C24:0 LacCer	956.7402	956.85	974.75077	974.85	996.73274	996.86

Figures and figure legends

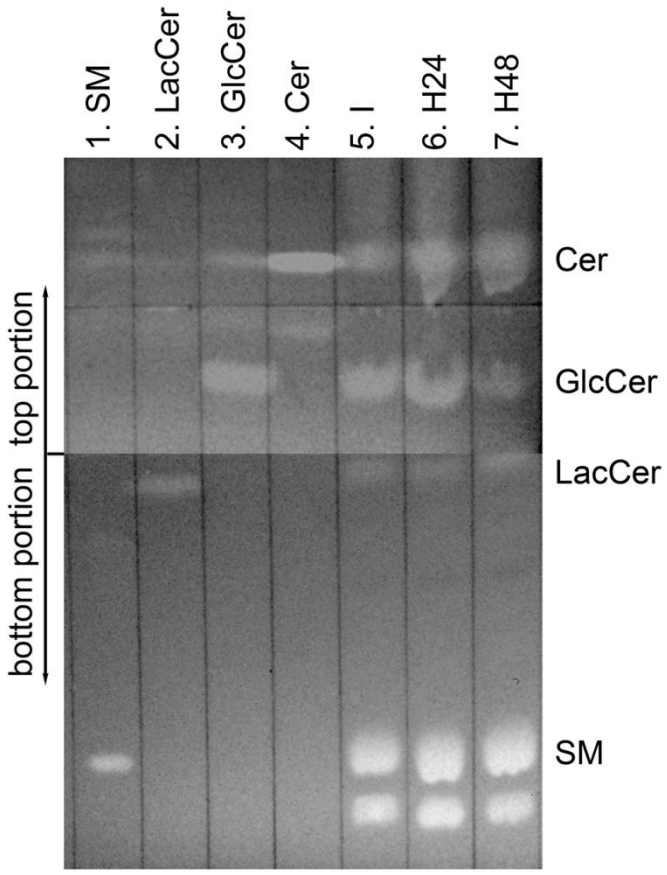

FIGURE 1. Thin-layer chromatogram stained with primuline. Sphingolipids were separated by a two-step TLC, as described in "Materials and Methods". The two portions of the plate (bottom and top) are shown. Lanes (1-4) contain lipid standards (SM, d18:1/12:0 N-lauroyl-D-erythro-sphingosylphosphorylcholine; LacCer, d18:1/12:0 D-lactosyl-ß-1,1' N-laurosyl-D-erythro-sphingosine; GlcCer, d18:1/18:0 D-glucosyl-ß-1,1' N-stearoyl-D-erythro-sphingosine; Cer, d18:1/12:0 N-lauroyl-D-erythrosphingosine). Lanes (5-7) contain sphingolipids extracted from cells cultured under isotonicity (I, lane 5), hypertonicity for 24 h (H24, lane 6) and hypertonicity for 48 h (H48, lane 7). SM, sphingomyelin; LacCer, lactosylceramide; GlcCer, glucosylceramide; Cer, ceramide.

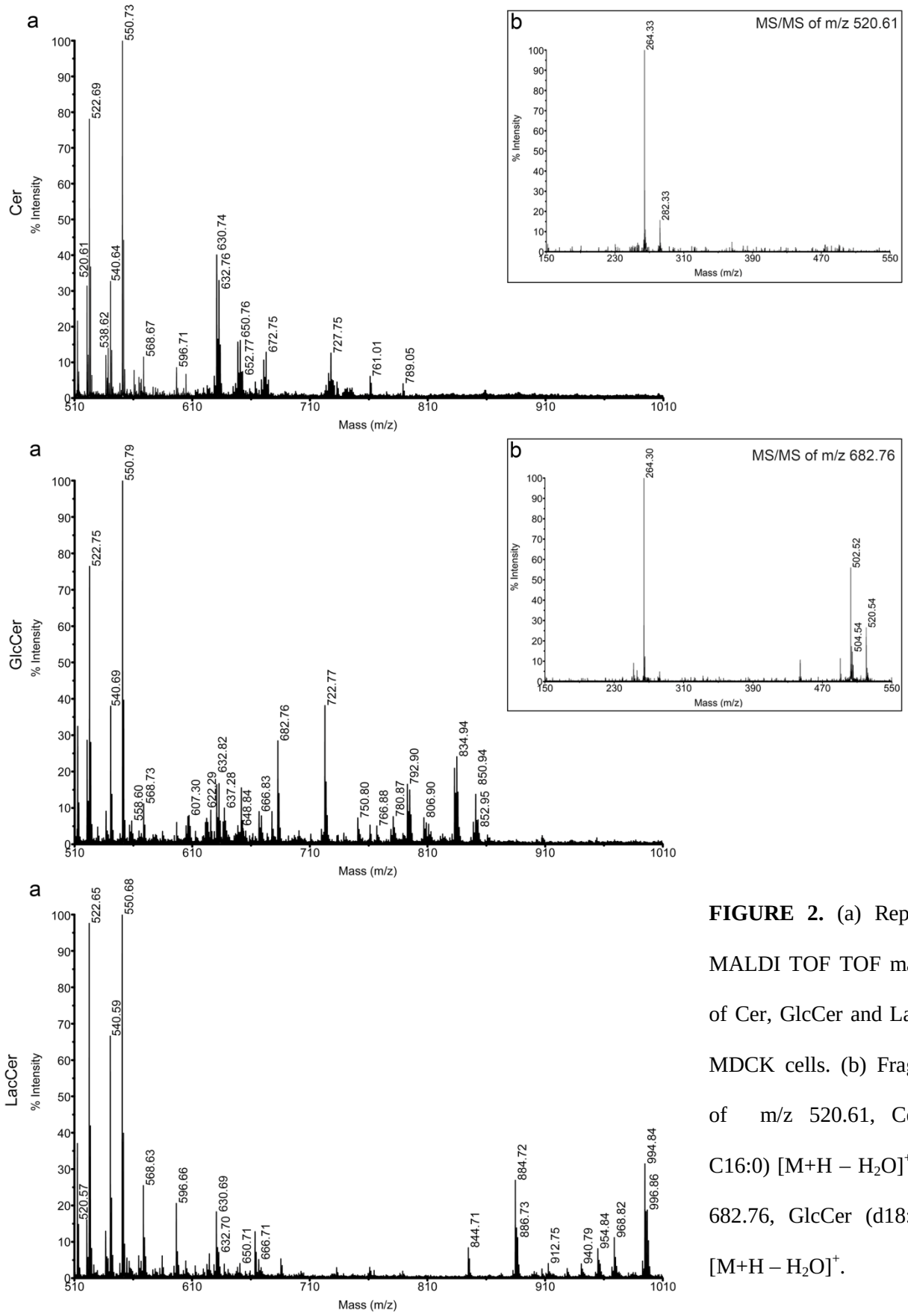

FIGURE 2. (a) Representative MALDI TOF TOF mass spectra of Cer, GlcCer and LacCer from MDCK cells. (b) Fragmentation of m/z 520.61, Cer (d18:1-C16:0) $[M+H - H_2O]^+$; and m/z 682.76, GlcCer (d18:1- C16:0) $[M+H - H_2O]^+$.

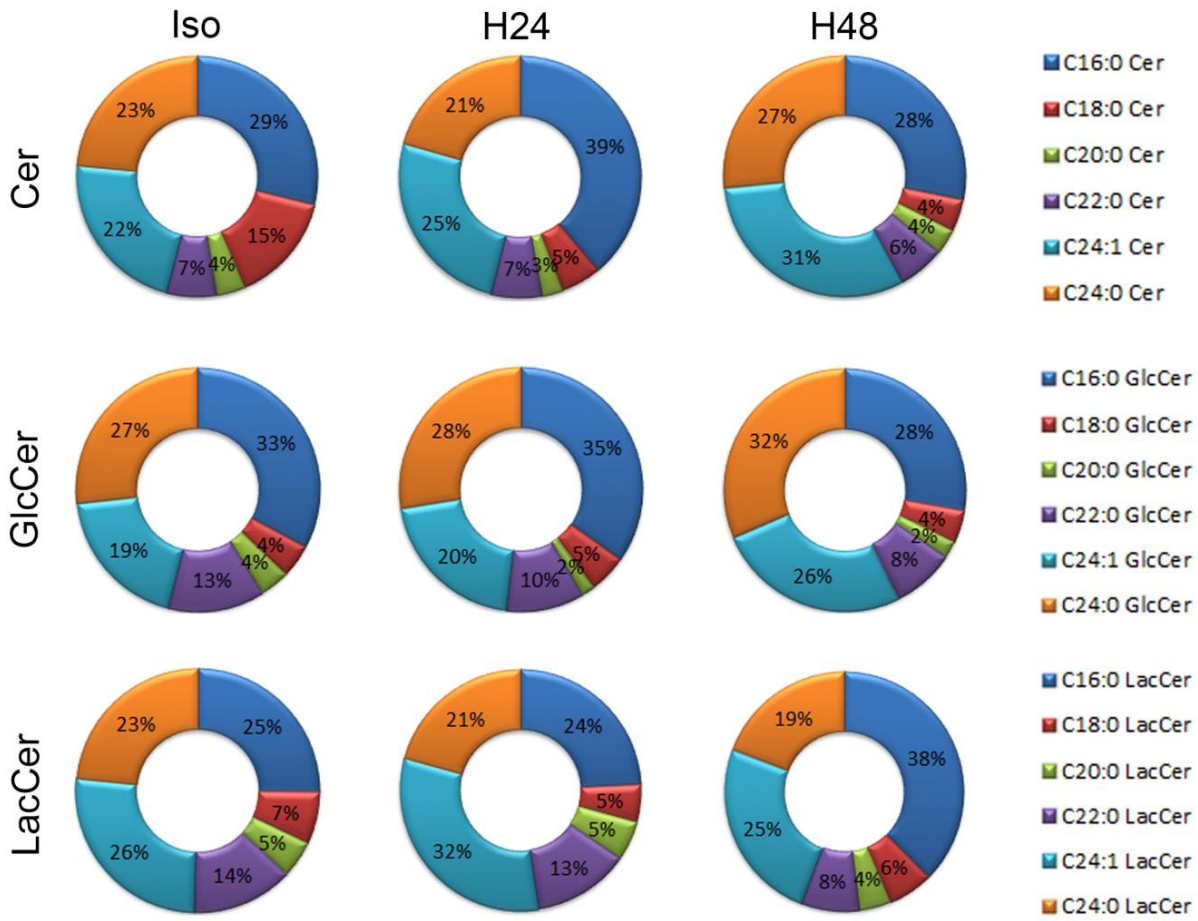

FIGURE 3. Pie chart panels for the percent distribution of acyl chains in Cer, GlcCer and LacCer in cells cultured under isotonicity (Iso), hypertonicity for 24 h (H24) and hypertonicity for 48 h (H48).

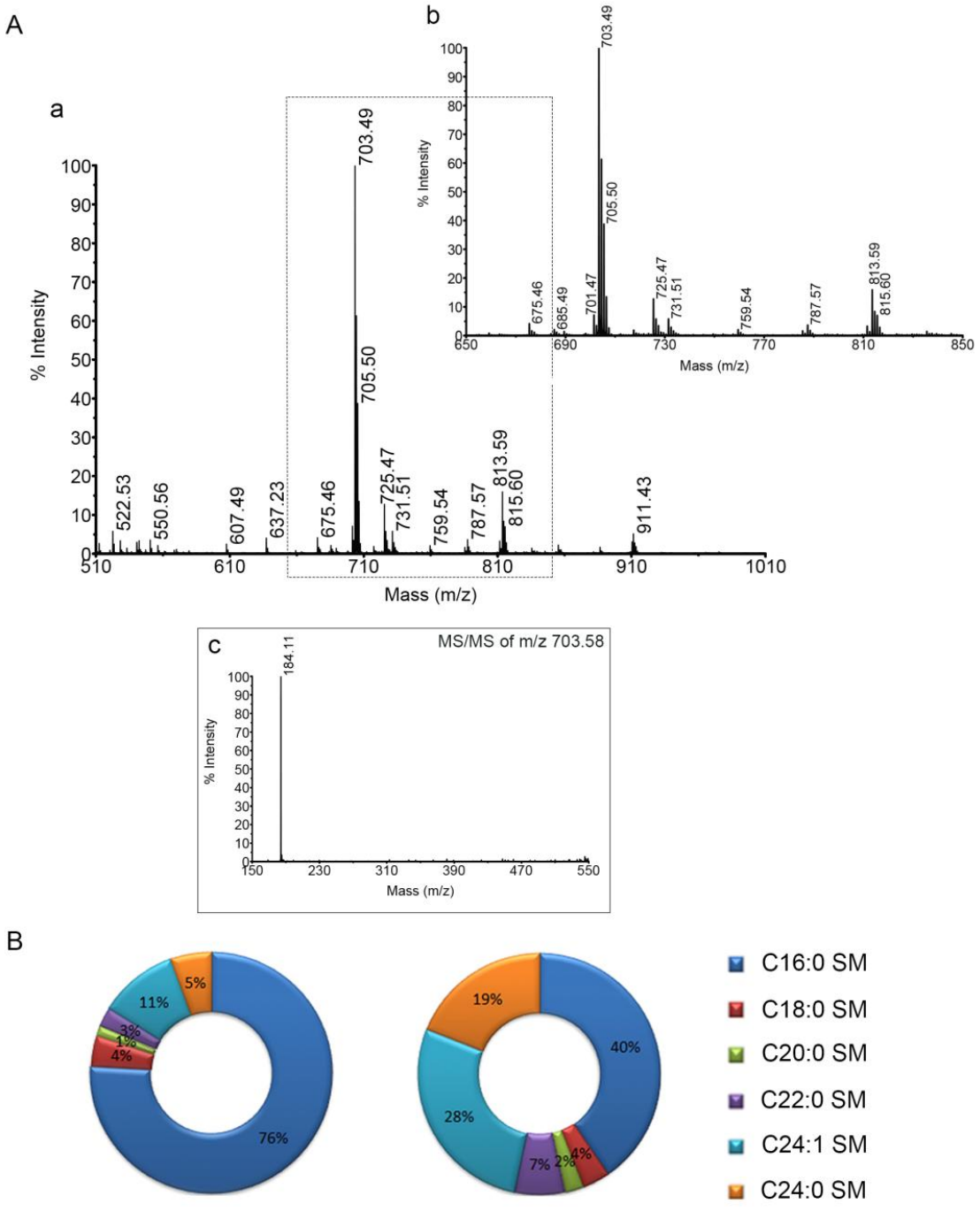

FIGURE 4. A (a): Representative MALDI TOF TOF mass spectra of SM from MDCK cells. (b) Magnification of the 650 -850 m/z range (dashed line). (c) Fragmentation of m/z 703.58, SM (d18:1-C16:0) $[M+H]^+$. B: Pie charts for the percent distribution of acyl chains in SM in cells cultured under isotonicity (left) and hypertonicity (right).

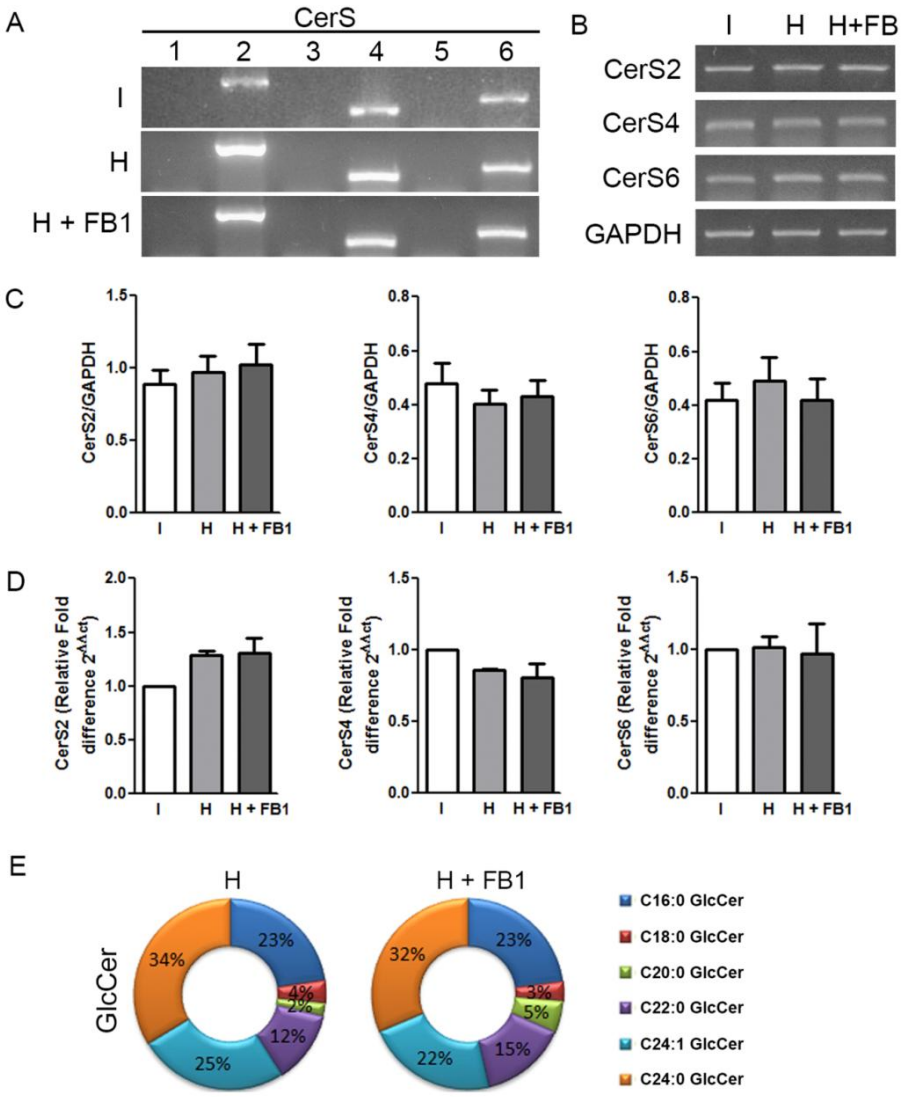

FIGURE 5. Expression of CerSs in cells cultured under isotonicity (I), hypertonicity (H) and hypertonicity in the presence of Fumonisin B1 (H + FB1). A: Representative agarose gel electrophoresis illustrating Reverse Transcription PCR (RT-PCR) products of CerS1-6 after 40 cycles of amplification. B: RT-PCR products of CerS2, CerS4, CerS6 and GAPDH by RT-PCR in adjusted conditions of amplification to detect changes in mRNA expression. C: Relative expression of CerS2, CerS4 and CerS6 mRNA analyzed by RT-PCR. D: Relative expression of CerS2, CerS4 and CerS6 mRNA quantified by Real Time PCR. The data represent the mean ± SEM from three independent experiments. E: Pie charts for the percent distribution of acyl chains in GlcCer in cells cultured under hypertonicity (left) and hypertonicity in the presence of FB1 (right).

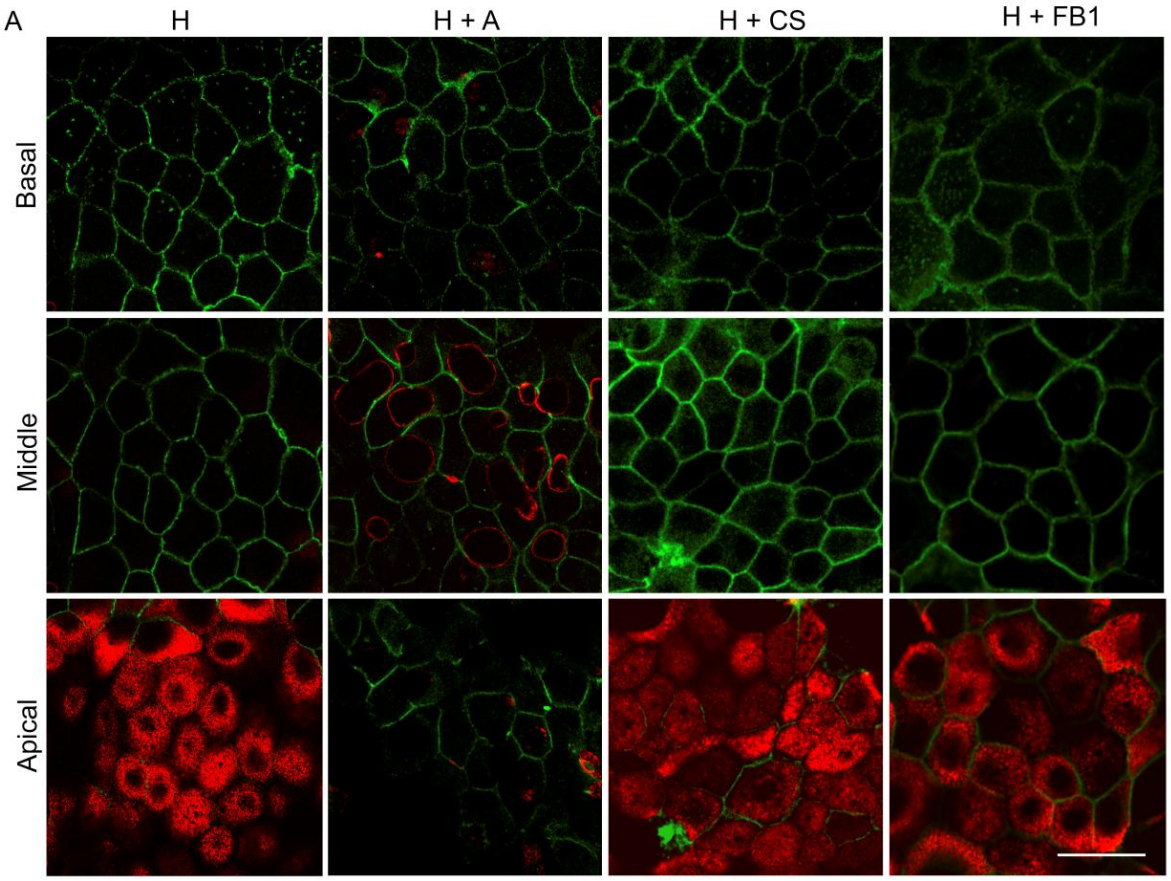

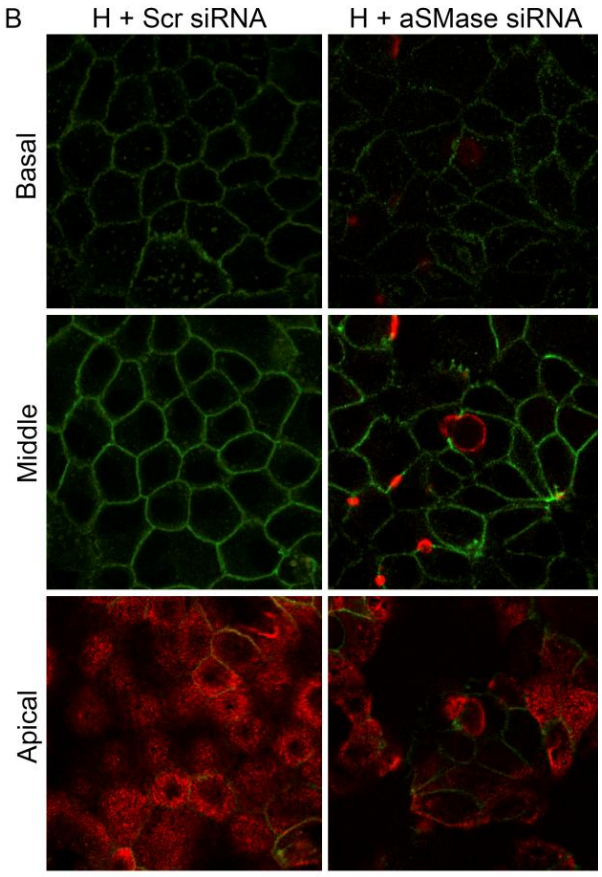

FIGURE 6. A. Immunofluorescence of MDCK cells cultured under hypertonicity (H), in the presence of amitriptyline (H + A), L-cycloserine (H + CS) and Fumonisin B1 (H + FB1). Confluent monolayers of MDCK cells incubated under hypertonicity in the presence or absence of the inhibitors were stained for gp135 (red) and α catenin (green) and imaged by confocal microscopy. Representative optical sections from the bottom (Basal), middle and top (Apical) of the monolayers are shown. B. MDCK cells were transfected with scrambled siRNA (control) or aSMase siRNA, then subjected to hypertonicity for 48h and stained as in A. Scale bar represents 30µm.

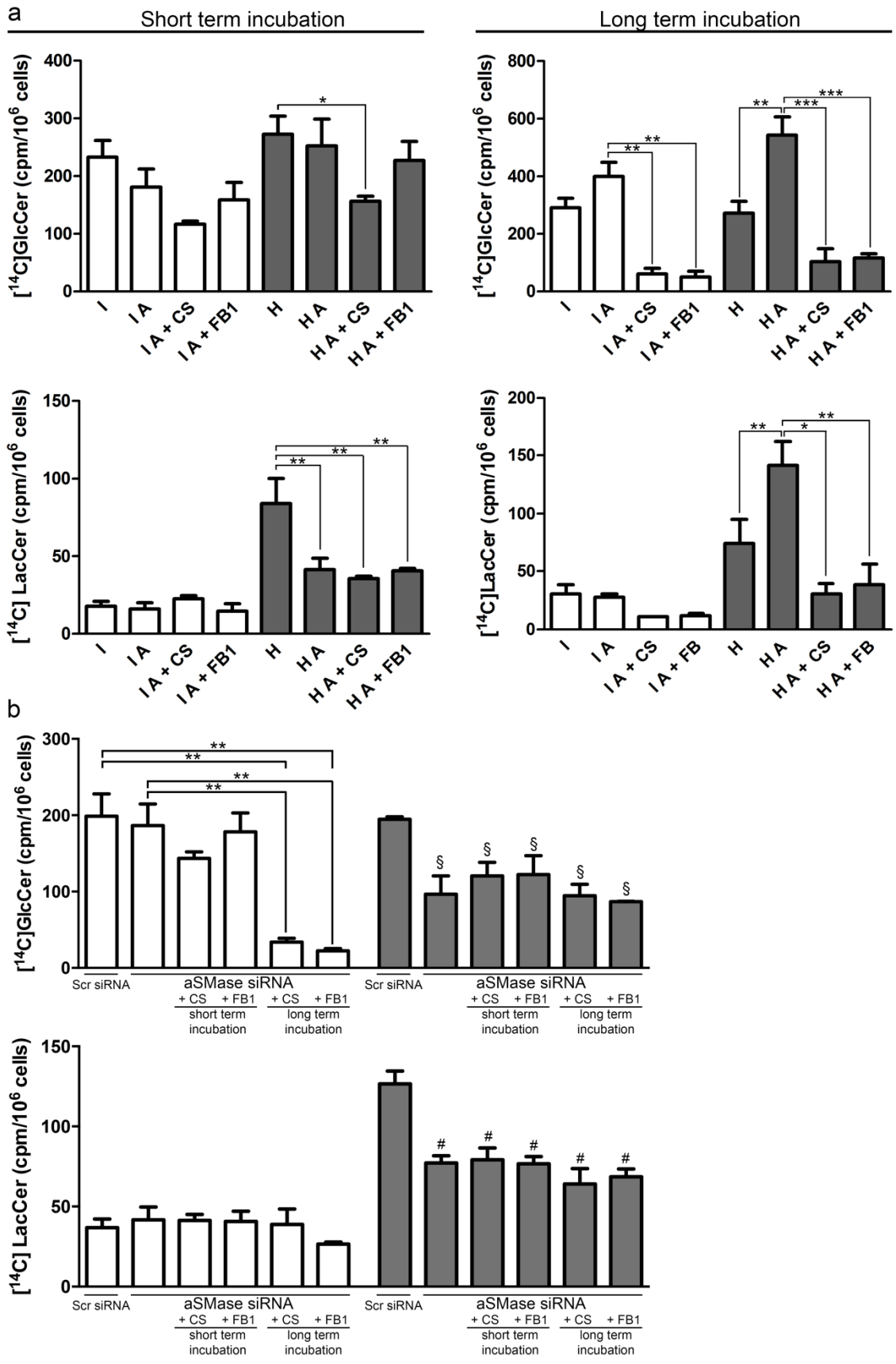
a
Short term incubation
Long term incubation
[14C]GlcCer (cpm/10^6 cells)
[14C] LacCer (cpm/10^6 cells)
[14C]LacCer (cpm/10^6 cells)
I
I A
I A + CS
I A + FB1
I A + FB
H
H A
H A + CS
H A + FB1
H A + FB
b
Scr siRNA
aSMase siRNA
+ CS
+ FB1
short term incubation
long term incubation

FIGURE 7. Effect of the inhibition of sphingolipid synthesis pathways in the metabolism of GlcCer and LacCer. (a) MDCK cells were incubated under isotonicity (I) or hypertonicity (H) in the presence or absence of amitriptyline (A), amitriptyline and L-cycloserine (A + CS) or amitriptyline and Fumonisin B1 (A + FB1) and radiolabeled for 5 h with [^{14}C]galactose. In the short-term incubation, the inhibitors were added 1 h before [^{14}C]galactose, whereas in the long-term incubation, the inhibitors were added 1 h before the addition of the hypertonic medium. Radiolabeled lipids were extracted and quantified as described in "Materials and Methods". (b) MDCK cells transfected with scrambled siRNA (Scr siRNA, control) or aSMase siRNA were incubated under isotonicity (I, white bars) or hypertonicity (H, gray bars) in the presence or absence L-cycloserine and Fumonisin B1 and radiolabeled with [^{14}C]galactose as in (a). The data represent the mean ± SEM from three independent experiments (*, $p<0.05$; **, $p<0.01$; ***, $p<0.001$; §, $p<0.05$ *vs* H Scr siRNA; #, $p<0.01$ *vs* H Scr siRNA, one-way ANOVA followed by Newman–Keuls multiple comparison test).